DOI: 10.13009/EUCASS2023-572
Aerospace Europe Conference 2023 – 10TH EUCASS – 9TH CEAS

Stability Characteristics of a Single Injector Combustor through Acoustic Solutions with Large Eddy Simulated Heat Sources

Musa Onur Ozturkmen[⋆,*,†] *and Yusuf Ozyoruk*[⋆]
[⋆] *Middle East Technical University*
Aerospace Engineering, Ankara, 06800, Turkey
[*] *Roketsan Missiles Inc.*
Elmadag, Ankara, 06780, Turkey
onur.ozturkmen@metu.edu.tr · yusuf.ozyoruk@ae.metu.edu.tr
[†]Corresponding author

Abstract
The stability characteristics of the experimental combustion chamber known as CVRC (Continuously Variable Resonance Chamber) in literature are investigated through frequency domain solutions of the nonhomogeneous wave equation with heat sources that are computed by large eddy simulation. The heat sources are represented by flame transfer functions and the discretized nonhomogeneous wave equation is cast into a non-linear quadratic eigenvalue problem which is first linearized, and then solved iteratively. By varying the oxidizer post length, the combustion chamber exhibits different stability characteristics due to acoustic and combustion interactions. An oxidizer post length of 13.97 cm is chosen for the study. The computed results exhibit consistent characteristics with those from literature.

1. Introduction

Combustion instabilities in propulsion systems continue to pose significant challenges in achieving efficient and reliable operation. These instabilities, characterized by unsteady and self-sustained oscillations in the combustion process, can lead to detrimental effects such as reduced performance, undesirable vibrations, increased emissions, and even catastrophic failure.[4,28,31] Consequently, researchers and engineers have been actively investigating various experimental and numerical methods to better understand and control these instabilities.[6,13,17,30]

Advances in computational fluid dynamics (CFD) and combustion modeling have influenced the study of combustion instabilities in liquid rocket engines in recent years. By simulating the complex fluid flow and combustion processes within the engine, numerical models allow researchers to analyze the intricate interplay between factors such as fuel injection, flame propagation, acoustic coupling, and heat transfer.[2,12,14,16,38] Even though these complicated processes in the combustion chamber may be simulated using large eddy simulation (LES) and may capture its unstable behavior, LES does not provide a detailed understanding of why the combustion chamber is unstable.[28] This may be compensated by the development of thermoacoustic codes. Their ability to simulate the complex interactions between the unsteady combustion process and the acoustic waves provides essential insights into the stability characteristics of the engine.

The thermoacoustic solvers are usually based on the linearized set of conservation equations for fluid flow. Examples include the linearized-Euler equation,[25,30,33] and the wave equation often known as the Helmholtz equation.[24,26,27] The Helmholtz equation provides a mathematical framework to describe the behavior of acoustic waves and their interactions with the surrounding fluid and boundaries of the combustion chamber. Solving the Helmholtz equation requires appropriate source terms for the flame response and boundary conditions, which are typically derived from the specific geometry and acoustic properties of the rocket engine. Properly accounting for these source terms are essential for accurate prediction and analysis of combustion instabilities.

Acoustic impedance boundary conditions are mathematical representations that describe the interaction of acoustic waves with solid boundaries. In the context of liquid rocket engines, these boundaries typically encompass the combustion chamber liner, injector plate, and nozzle throat, among others. The combustion process within the chamber generates high-pressure oscillations, resulting in the production of acoustic waves that propagate through the surrounding medium. When these waves reach the boundaries, they experience impedance mismatch, leading to wave reflections, transmission, and attenuation.

DOI: 10.13009/EUCASS2023-572

The Helmholtz equation separates acoustic and combustion solutions achieved using a flame transfer function (FTF). The FTF serves as a mathematical tool to describe the dynamic relationship between the heat release rate fluctuations and the pressure fluctuations in a combustor. It quantifies how changes in the flame shape and position, caused by pressure fluctuations, influence the heat release rate, and how these variations feed back into the pressure fluctuations. In other words, the FTF provides a quantitative measure of the amplification or attenuation of oscillations at different frequencies by determining the transfer function between the pressure and heat release rate fluctuations. The various experimental and computational techniques are applied to determine the FTF, including dynamic pressure measurements, optical diagnostics,[7,8,22] theoretical formulations[3,19,20] and numerical simulations.[36,37]

In this study, we delve into the application of the Helmholtz equation in the prediction of combustion instabilities for a single injector experimental combustor known as the Continuously Variable Resonance Chamber (CVRC).[23,35,40] The flame transfer functions produced from large eddy simulation, as well as the accompanying impedance boundary conditions, are used as source terms in the nonhomogeneous Helmholtz equation. The parts that follow begin with a brief description of the non-homogeneous wave equation and how to handle the boundary and heat sources. The findings of acoustic simulations are then presented and discussed.

2. Methodology

The wave equation for a generic combustion chamber is typically derived by decomposing the governing equations of the combustion system into linearized form, assuming small perturbations around a steady-state operating condition, and neglecting nonlinear terms. The derived wave equation is transformed into the frequency domain by rewriting each time dependent fluctuation term as $Q'(\mathbf{x}, t) = \hat{Q}(\mathbf{x}, \omega)\ \exp(+i\omega t)$ with defining the wavenumber as $k \equiv \omega/\bar{c}_0$. Then the obtained equation is called the Helmholtz equation and reads,

$$k^2 \hat{p}(\mathbf{x}, k) + \frac{c_0^2(\mathbf{x})}{\bar{c}_0^2}\rho_0(\mathbf{x})\nabla \cdot \left(\frac{1}{\rho_0(\mathbf{x})}\nabla \hat{p}(\mathbf{x}, k)\right) = \hat{h}(\mathbf{x}, k), \tag{1}$$

and the problem is closed with the boundary conditions,

$$\mathbf{n}(\mathbf{x}) \cdot \nabla \hat{p}(\mathbf{x}, k) = -\hat{f}(\mathbf{x}, k) \tag{2}$$

where c_0 and $\bar{c}_0$ represent the local and a reference (e.g. chamber-wide average) speed of sound, respectively. h represents all the linear and nonlinear interactions among the chamber acoustics, combustion, and mean flow and, f represents the sources due to the boundary conditions. For the details of the conservation equations and source terms, readers are referred, for example, to Culick.[6]

With the assumption of low Mach number in the chamber and the combustion instability being driven solely by the unsteady heat release, the right hand side of the nonhomogenous wave equation simplifies. Linear motions under the effects of unsteady heat release are governed in the frequency domain by the Helmholtz equation and equation (1) can be rewritten as,

$$k^2 \hat{p}(\mathbf{x}, k) + \frac{c_0^2(\mathbf{x})}{\bar{c}_0^2}\rho_0(\mathbf{x})\nabla \cdot \left(\frac{1}{\rho_0(\mathbf{x})}\nabla \hat{p}(\mathbf{x}, k)\right) = -\frac{\gamma_0(\mathbf{x}) - 1}{\bar{c}_0}\, i\, k\, \hat{q}(\mathbf{x}, k) \tag{3}$$

Note that the wavenumber, k, is complex valued when the sources are non-zero. The frequency of oscillations is defined by the real part of the wavenumber, whereas the growth rate of oscillations is defined by the imaginary part. The stability of a mode is determined by the sign of its imaginary part. A negative sign (recall usage of the $\exp(+i\omega t)$ convention) denotes an unstable mode.

The discretization of the Helmholtz equation is carried out by a linear finite element method and the problem is converted to an eigenvalue problem by proper treatment of the boundary conditions and heat sources. The impedance boundary condition, i.e., the boundary source term, $\hat{f}$ can be expressed in terms of pressure and normal velocity perturbations, which are related by the linear momentum equation and can be written as,

$$\mathbf{n}(\mathbf{x}) \cdot \nabla \hat{p}(\mathbf{x}, k) = -\frac{ik\rho_0(\mathbf{x})/\bar{\rho}_0}{Z^*(\mathbf{x}, k)}\hat{p}(\mathbf{x}, k). \tag{4}$$

Furthermore, the dynamic interaction between the combustion process and the acoustic oscillations within the combustion chamber is described by using the flame transfer functions. The flame transfer function relates unsteady heat release with respect to velocity fluctuations at a reference point, and mathematically can be written as:

$$F(\mathbf{x}, k) = \frac{\hat{q}(\mathbf{x}, k)}{\hat{u}(\mathbf{x}_{ref}, k)} \tag{5}$$

DOI: 10.13009/EUCASS2023-572

The velocity perturbation in equation (5) is conveyed to the pressure perturbation via the local momentum equation at the reference point, similar to the impedance condition. Then, the heat source, $\hat{q}$, may be expressed as,

$$\hat{q}(\mathbf{x}, k) = F(\mathbf{x}, k)\frac{\mathbf{n}_{\text{ref}} \cdot \nabla\hat{p}(\mathbf{x}_{\text{ref}}, k)}{\rho_0(\mathbf{x}_{\text{ref}})}. \tag{6}$$

The discretized Helmholtz equation for a given computational domain, together with the formulation of the flame transfer function and impedance boundary conditions, yields the nonlinear quadratic eigenvalue problem:

$$k^2\,\mathbf{M}\,\hat{\mathbf{p}} + k\,\mathbf{C}^{(b)}(k)\,\hat{\mathbf{p}} + \left(\mathbf{K}^{(c)}(k) + \mathbf{K}^{(n)}\right)\hat{\mathbf{p}} = 0 \tag{7}$$

where $\mathbf{M}$, $\mathbf{C}$, and $\mathbf{K}$ are the coefficient matrices, $\hat{\mathbf{p}}$ is the pressure perturbation vector, and the superscript (b) represents the matrices formed due to the impedance boundary conditions, (c) represents the matrices due to heat release, and the superscript (n) is associated with the matrix that arises in the standard, natural problem.

The nonlinear quadratic eigenvalue problems are often solved as generalized eigenvalue problems by applying linearization techniques. Different linearization techniques have been applied for the combustion instability problems such as fixed point iteration,[24] and relaxation with fixed point iteration.[34] The authors have also proposed to use linearization based on the first-order Taylor series expansion of the frequency dependent coefficient matrices resulting from frequency dependent source terms.[26] This latter, gradient-based linearization, approach is used in this work to achieve linearization. To linearize the nonlinear terms in this approach, the coefficient matrices are expanded into first-order Taylor series about the previously computed wavenumber. Substituting the expansions into the equation (7), and collecting the same order terms in k together, the following linearized form of the is obtained:

$$\begin{aligned} k_{\ell+1}^2\left[\mathbf{M} + \alpha_b\frac{d\mathbf{C}^{(b)}(k)}{dk}\right]_{k=k_\ell}\hat{\mathbf{p}} + k_{\ell+1}\left[\left(\mathbf{C}^{(b)}(k) - k\alpha_b\frac{d\mathbf{C}^{(b)}(k)}{dk}\right) + \alpha_c\frac{d\mathbf{K}^{(c)}(k)}{dk}\right]_{k=k_\ell}\hat{\mathbf{p}} \\ + \left[\left(\mathbf{K}^{(c)}(k) - k\alpha_c\frac{d\mathbf{K}^{(c)}(k)}{dk}\right) + \mathbf{K}^{(n)}\right]_{k=k_\ell}\hat{\mathbf{p}} = 0. \end{aligned} \tag{8}$$

where α_b and α_c are two factors introduced for limiting the gradients. For the results presented below using this gradient based linearization approach $\alpha_b = 1$ and $\alpha_c \approx 0.25$ were used. $\alpha_b = 0$ and $\alpha_c = 0$ correspond to the fixed-point iteration approach.

The above quadratic eigenvalue problem can be solved using complex arithmetic libraries. ARPACK[21] and SLEPc[18] are two widely used libraries for the solution of many different types of eigenvalue problems. The in-house Helmholtz solver makes use of both. However, the results provided in this study were achieved by utilizing the latter.

3. Results and Discussion

In this section, the experimental test setup called as Continuously Variable Resonance Chamber (CVRC)[23,35,40] is solved with frequency dependent heat sources and impedance boundary conditions as a benchmark to assess the reliability of the code predictions. The numerical setup and study are discussed in the following subsections.

3.1 Problem definition and geometry

The combustion chamber has a cylindrical body measuring 38.1 cm in length and 4.5 cm in diameter. A coaxial injector introduces fuel and oxidizer into the combustion chamber. The length of the oxidizer post can be adjusted between 8.89 cm and 19.05 cm. To achieve high pressure inside the combustion chamber, the combustion chamber is finished with a converging diverging nozzle. Figure 1 depicts the dimensions of the geometry employed in the present study. More information on the experimental setup and process can be obtained at.[39]

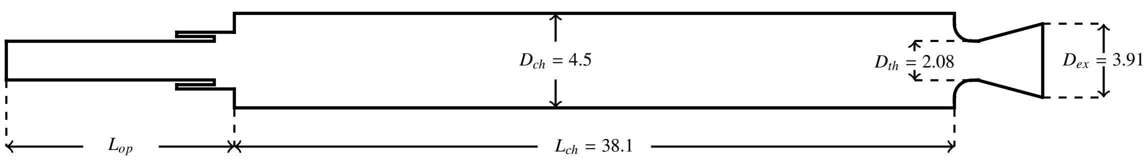

Figure 1: Geometry of the CVRC (dimensions are in cm).

DOI: 10.13009/EUCASS2023-572

The fuel is composed entirely of gaseous methane. In terms of mass fraction, the oxidizer is a gaseous mixture made up of 42% oxygen and 58% water. The oxidizer and fuel are injected into the chamber at 1030 K and 300 K, respectively.

The CVRC has a variable oxidizer injector length. Due to different injector post length, the combustion chamber exhibits different stability characteristics through acoustic and combustion interactions. According to the stability map documented in Selle et al.,[32] the unstable region is encountered when oxidizer injector post length change between 9.5 cm to 16 cm. Hence, from this region, the oxidizer post length of $L_{op} = 13.97$ cm is chosen for this study.

3.2 Numerical Approach

3.2.1 Domain and boundary conditions

The solution approach described in preceding section is applied to the geometry shown in 1. The geometry is approximated axisymmetrically by eliminating the nozzle and fuel inlet because the fuel inlet is too small and behaves similarly to a rigid wall boundary. The oxidizer post length is artificially truncated by moving the inlet boundary downstream to obtain a frequency dependent boundary condition. The oxidizer post is shortened by 0.0635 m. The computational domain used in acoustic calculations is depicted in Figure 2.

Figure 2: Truncated computation domain of the CVRC setup.

The inlet impedance boundary condition is calculated theoretically using knowing that the oxidizer injector chokes the flow to the oxidizer post,[11] resulting in a constant mass flow rate at the injector post inlet. The nondimensional inlet impedance is obtained as,

$$Z^*_{\mathrm{in}} = -\frac{1}{\mathbf{n}\cdot\mathbf{M}}\bigg|_{\mathrm{in}}. \tag{9}$$

From equation (9), the inlet impedance is calculated as $Z^*_{\mathrm{in}} = 2.78$. This estimated value is not used directly because it is only valid at the full domain's inlet. The value of the truncated domain's inlet, Z^{*T}_{in}, is obtained using the impedance translation formula for a translation length of ΔL. Note that this translation makes the left boundary of the computational domain frequency dependent.

The outlet impedance condition at the downstream end of the chamber, is determined by solving the frequency-domain linearized Euler equations in quasi-one dimensional form. The calculations commence at the nozzle throat, where the impedance is defined due to the choked condition. Figure 3 depicts the computed outlet impedance values. The outlet impedance is clearly critical for the first few longitudinal modes due to significant reflections from the boundary. More information on the calculation of impedance boundary conditions can be found in reference.[26]

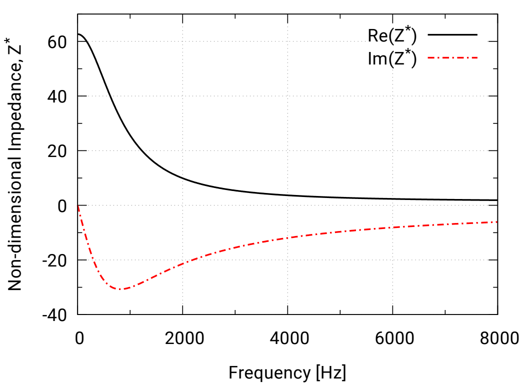

Figure 3: The calculated outlet impedance.

DOI: 10.13009/EUCASS2023-572

3.2.2 Flame transfer function

Remember that the thermoacoustic instability in a chamber is driven by unsteady heat release combined with the chamber acoustic field, and the unsteady heat release is incorporated using the flame transfer functions. The FTFs utilized in the calculations are derived from large eddy simulations (LES).

LES is conducted to accurately determine the heat release distribution inside the chamber for the defined problem in section 3.1. The simulations are done using CFD++ software from Metacomp Technologies.[1] Despite the fact that turbulent structures are essentially three-dimensional, the study is conducted in axisymmetric mode. In the literature, a similar approach is utilized for modeling longitudinal instability.[32] This method decreases the calculation time and enables a quick evaluation of the thermoacoustic instability of the chamber. The chemistry is modeled with a reduced reaction set of BFER[9] includes two-step reactions with five species (CH4, O2, H2O, CO, and CO2).

The LES results illustrate the overall stability of the combustion chamber. Figure 4 depicts the power spectral density (PSD) of the self-sustained pressure fluctuations collected at the oxidizer inlet. According to this result, the first longitudinal mode of the chamber with the oxidizer post length of 13.97 cm is unstable with a frequency of 1565.1 Hz.

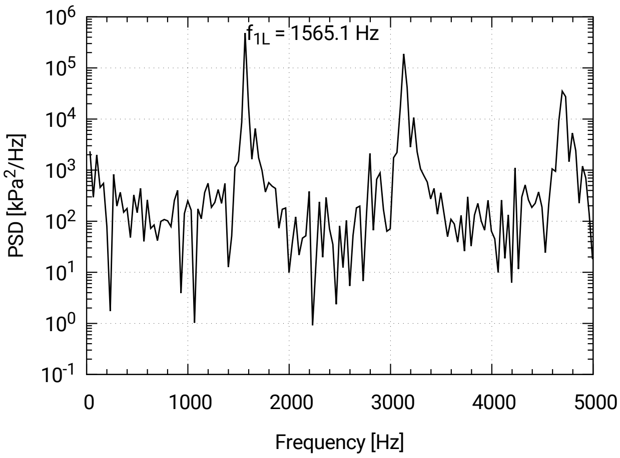

Figure 4: Power spectral density of the pressure fluctuation of the numerical probe at the oxidizer inlet of CVRC with $L_{op} = 13.97$ cm.

The FTF distribution is extracted in both frequency and space using time resolved data collected over the computational domain. During simulation, a time dependent data length of 300300 is collected at a sampling rate of $\Delta t_s = 5 \times 10^{-6}$ sec. This sampling rate yields a frequency resolution of 33.3 Hz. The data is processed using an in-house post processing code based on the VTK[29] and FFTW[10] libraries to obtain the Fourier transforms of the unsteady heat release in the entire domain, $\hat{q}(\mathbf{x}, \omega)$, and axial velocity fluctuations at the reference point, $\hat{u}(\mathbf{x}_{\text{ref}}, \omega)$. Then, the FTFs are constructed by dividing the Fourier transform of the unsteady heat release by the Fourier transform of velocity fluctuation at a reference point, as defined by equation (5).

The $n - \tau$ method, initially defined by Crocco,[5] can also be used to formulate the flame transfer function, with the main assumption based on experiments that the flame surface varies linearly with the velocity in front of the flame. The flame transfer function can be rebuilt using the $n - \tau$ method as follows:

$$F(\mathbf{x}, \omega) = n(\mathbf{x}, \omega) e^{-i\omega\tau(\mathbf{x},\omega)} \tag{10}$$

where $n(\mathbf{x}, \omega)$ represents the interaction index and $\tau(\mathbf{x}, \omega)$ represents the time delay. In general, both are affected by the frequency of oscillations. The interaction index quantifies the magnitude of the flame's response to a perturbation. Meanwhile, the time delay describes how long it takes for the flame response to come out following a disturbance at the reference location. The fields of interaction index and time delay are obtained as:

$$\begin{aligned} n &= |F(\mathbf{x}, \omega)| \\ \tau &= \frac{\phi(\mathbf{x}, \omega)}{\Re(\omega)} \qquad \text{if } \phi(\mathbf{x}, \omega) \geq 0 \\ &= \frac{2\pi + \phi(\mathbf{x}, \omega)}{\Re(\omega)} \qquad \text{if } \phi(\mathbf{x}, \omega) < 0 \\ \phi(\mathbf{x}, \omega) &= \tan^{-1}\left(\frac{\Im(F(\mathbf{x}, \omega))}{\Re(F(\mathbf{x}, \omega))}\right) \end{aligned} \tag{11}$$

DOI: 10.13009/EUCASS2023-572

The computed fields of the interaction index, $n(\mathbf{x}, \omega)$, and time delay, $\tau(\mathbf{x}, \omega)$ are displayed in Figure 5 and Figure 6, respectively. Because of the division of small velocity fluctuations at the reference point (refer equation (5)), the magnitude of the interaction index increases as it moves away from the instability frequency. These high values do not contribute since the time delay is not effective in those regions.

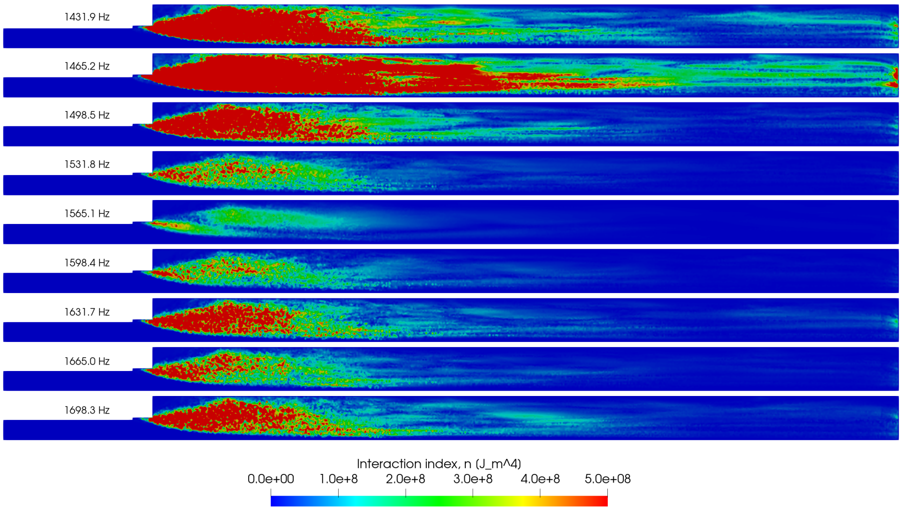

Figure 5: Frequency dependent interaction index distributions for the CVRC, L_{op} = 13.97 cm.

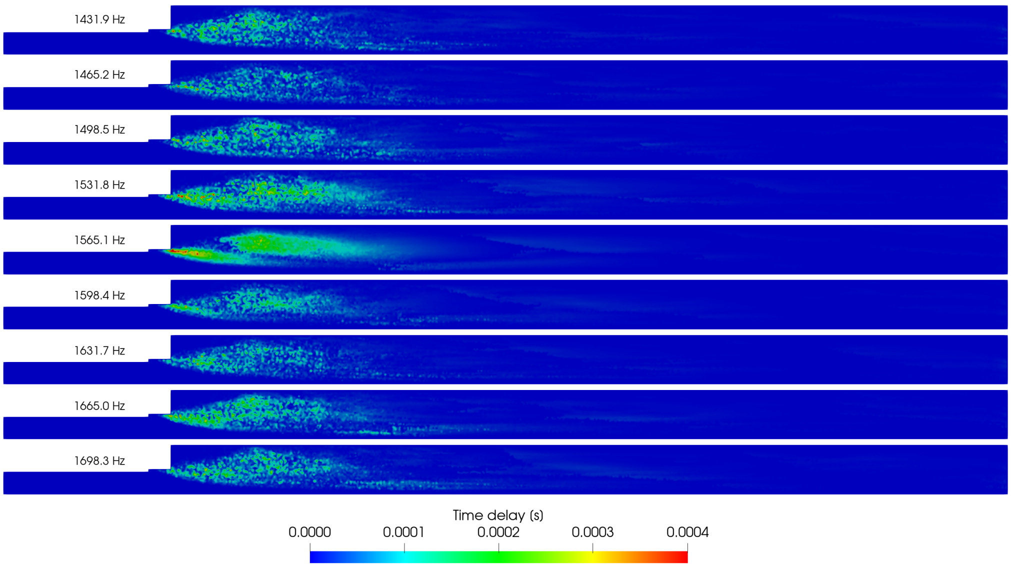

Figure 6: Frequency dependent time delay distributions for the CVRC, L_{op} = 13.97 cm.

Note also that the Helmholtz solver does not account for mean flow effects (due to the assumption that $M(x) << c_0$), whereas the LES inherently does. As a result, when solving the Helmholtz equation, the frequency dependent FTFs should be used with caution. The frequency dependent FTFs are introduced into the Helmholtz equation with a flow correction defined as $f_{M\neq0} = (1 - M^2_{\text{ave}})f_{M=0}$.

DOI: 10.13009/EUCASS2023-572

3.3 Results from the Helmholtz solver

This section works with the computational domain presented in Figure 2 and includes results based on the LES computed inlet impedance and the flame transfer functions. The FTFs used in the calculations have frequencies ranging from 1032.3 to 2997.0 Hz. The correction value is set to $M_{\mathrm{ave}} = 0.25$ during the inclusion of the FTFs.

Linearization methods are used in iterative calculations, and calculations begin with the solution of rigid boundaries. Figure 7 depicts the convergence histories for the first longitudinal mode of the CVRC. The gradient-based linearization appears to converge quickly, whereas the other techniques are more oscillatory. Similarly, the change of the frequency dependent inlet and outlet impedance boundaries with iterations are shown in Figure 8. When compared to other methods, using gradient-based linearization results in faster convergence of the impedance values.

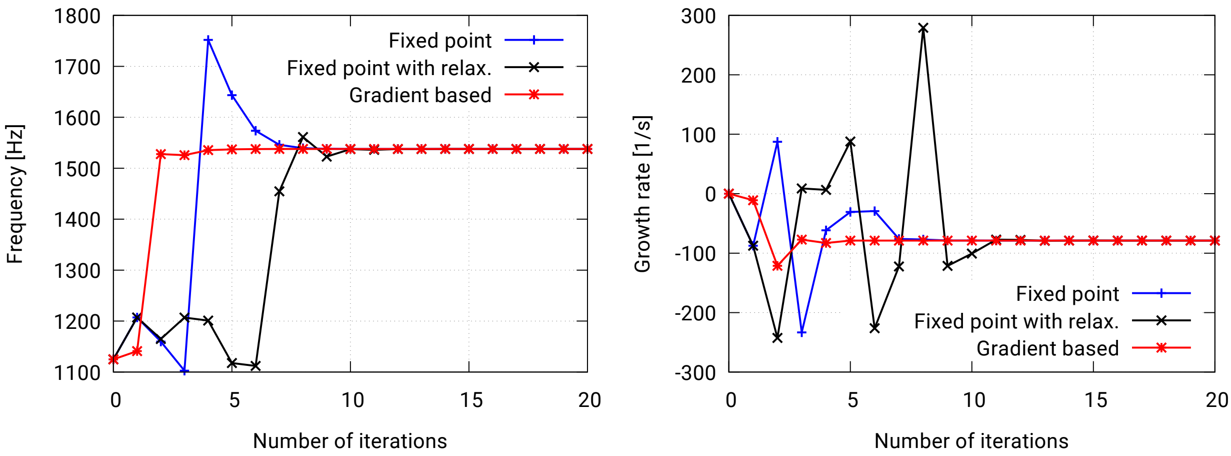

(a) Real part

(b) Imaginary part

Figure 7: Convergence behavior of the linearization methods for the first longitudinal mode.

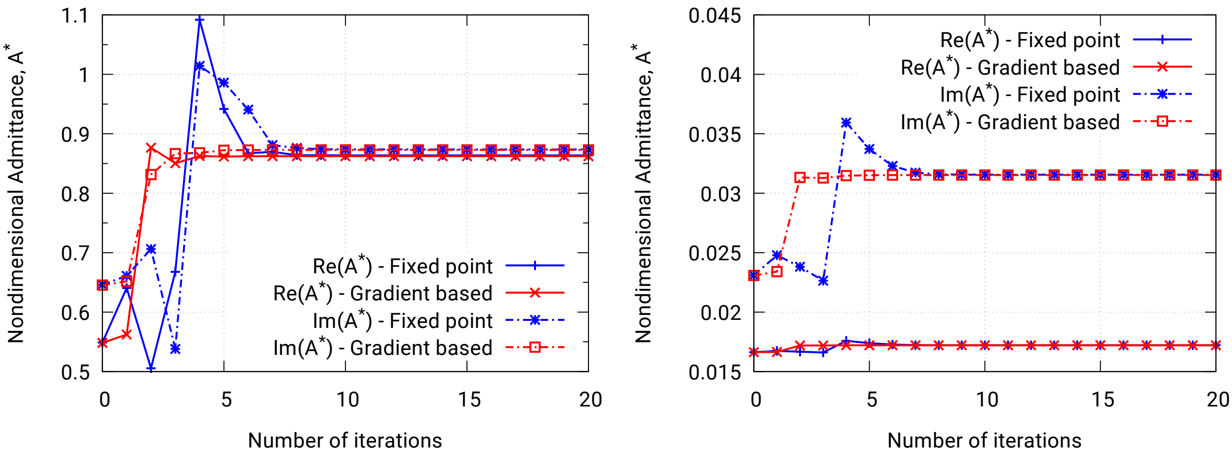

(a) Inlet

(b) Outlet

Figure 8: Iterative variation of the CVRC combustion chamber's inlet admittance (A^{*T}) and outlet admittance (A^{*}_{out}) for the first longitudinal mode.

Table 1 summarizes and compares the numerical values of the converged frequency from the acoustic solver using FTFs to literature data. Both the frequency obtained directly from LES and those predicted by the acoustic solution employing the LES produced FTFs are both consistent with the literature data.

DOI: 10.13009/EUCASS2023-572

Table 1: Comparison of the obtained results for the first longitudinal mode frequencies with literature data for the CVRC setup with L_{op} = 13.97 cm.

Reference	**Frequency** (Hz)	**Growth rate** (1/s)
Experiment[41]	1350	
AFRL, 2D axis. - 4 Step[15]	1460	-
AFRL, 2D axis. - 1 Step[15]	1650	-
AFRL, 3D - 1 Step [15]	1550	-
Present 2D axis. - 2 Step LES	1565	-
Present acoustic solution	1538	-78

4. Conclusion

The purpose of this work is to numerically study stability characteristics of the combustion chamber known in literature as CVRC with a post oxidizer length of L_{op} = 13.97 cm through solutions of the Helmholtz equation with a frequency dependent heat sources and impedance boundary conditions. Large eddy simulations are used to obtain the heat source distributions, and the eigenvalue problem is constructed by finite element discretization of the Helmholtz equation with these sources. The resulting nonlinear quadratic eigenvalue problem is linearized by three different approaches, and solved iteratively. The computed frequencies for the CVRC with L_{op} = 13.97 cm presented showed consistent characteristics with those from literature. Also, the gradient based linearization approach resulted convergence in fewer iterations.

5. Acknowledgments

The numerical calculations presented in the current study were carried out in part using the TUBITAK ULAKBIM High Performance and Grid Computing Center (TRUBA resources). This work has also been supported by the Defence Industry Agency of Turkey.

References

[1] CFD++. https://www.metacomptech.com/.

[2] S. K. Beinke, J. S. Hardi, D. T. Banuti, S. K., B. B. Dally, and M. Oschwald. Experimental and numerical study of transcritical oxygen-hydrogen rocket flame response to transverse acoustic excitation. *Proceedings of the Combustion Institute*, 38(4):5979–5986, 2021.

[3] F. Biagioli, A. Innocenti, A. Lamraoui, and K. J. Syed. Analytical modelling of flame transfer functions for technically premixed flames. *International Journal of Spray and Combustion Dynamics*, 14(1-2):42–54, 2022.

[4] S. Candel, D. Durox, and T. Schuller. Flame interactions as a source of noise and combustion instabilities. 10th AIAA/CEAS Aeroacoustics Conference, 2004.

[5] L. Crocco. Aspects of combustion instability in liquid propellant rocket motors. part I. *J. American Rocket Society*, 21:163–178, 1951.

[6] F.E.C. Culick. Unsteady motions in combustion chambers for propulsion systems. AG-AVT-039, 2006.

[7] S. Ducruix, D. Durox, and S. Candel. Theoretical and experimental determinations of the transfer function of a laminar premixed flame. *Proceedings of the Combustion Institute*, 28(1):765–773, 2000.

[8] D. Durox, T. Schuller, N. Noiray, and S. Candel. Experimental analysis of nonlinear flame transfer functions for different flame geometries. *Proceedings of the Combustion Institute*, 32(1):1391–1398, 2009.

[9] B. Franzelli, E. Riber, M. SanjosÃ©, and T. Poinsot. A two-step chemical scheme for large-eddy simulation of kerosene-air flames. *Combustion and Flame*, 157:1364–1373, 2010.

[10] M. Frigo and S. G. Johnson. The design and implementation of FFTW3. *Proceedings of the IEEE*, 93(2):216–231, 2005. Special issue on “Program Generation, Optimization, and Platform Adaptation”.

DOI: 10.13009/EUCASS2023-572

[11] R. Garby. *Simulations of flame stabilization and stability in high-pressure propulsion systems*. PhD thesis, The University of Toulouse, 2013.

[12] R. Garby, L. Selle, and T. Poinsot. *Analysis of the impact of heat losses on an unstable model rocket-engine combustor using Large-Eddy Simulation*.

[13] J. S. Hardi, H. C. G. Martinez, M. Oschwald, and B. B. Dally. Lox jet atomization under transverse acoustic oscillations. *Journal of Propulsion and Power*, 30(2):337–349, 2014.

[14] Justin S. Hardi. *Experimental Investigation of High Frequency Combustion Instability in Cryogenic Oxygen-Hydrogen Rocket Engines*. PhD thesis, The University of Adelaide, 2012.

[15] M. E. Harvazinski. *Modeling Self-Excited Combustion Instabilities Using a Combination Of Two- And Three-Dimensional Simulations*. PhD thesis, Purdue University, 2012.

[16] M. E. Harvazinski, C. Huang, V. Sankaran, T. W. Feldman, W. E. Anderson, C. L. Merkle, and D. G. Talley. Coupling between hydrodynamics, acoustics, and heat release in a self-excited unstable combustor. *Physics of Fluids*, 27(4), 04 2015.

[17] G. Heilmann and T. Sattelmayer. On the convective wave equation for the investigation of combustor stability using fem-methods. *International Journal of Spray and Combustion Dynamics*, 14(1-2):55–71, 2022.

[18] V. Hernandez, J. E. Roman, and V. Vidal. SLEPc: A scalable and flexible toolkit for the solution of eigenvalue problems. *ACM Trans. Math. Software*, 31(3):351–362, 2005.

[19] K.T. Kim, J.G. Lee, B.D. Quay, and D.A. Santavicca. Spatially distributed flame transfer functions for predicting combustion dynamics in lean premixed gas turbine combustors. *Combustion and Flame*, 157(9):1718–1730, 2010.

[20] C. Kulsheimer and H. Buchner. Combustion dynamics of turbulent swirling flames. *Combustion and Flame*, 131(1):70–84, 2002.

[21] R. B. Lehoucq, D. C. Sorensen, and C. Yang. ARPACK User's Guide Solution of Large-scale Eigenvalue Problems with Implicitly Restarted Arnoldi Methods. SIAM, 3600 Market Street, Floor 6, Philadelphia, PA, 1998.

[22] T. Lieuwen and Y. Neumeier. Nonlinear pressure-heat release transfer function measurements in a premixed combustor. *Proceedings of the Combustion Institute*, 29(1):99–105, 2002. Proceedings of the Combustion Institute.

[23] K. J. Miller. Experimental study of longitudinal instabilities in a single element rocket combustor. Master's thesis, Purdue University, 2005.

[24] F. Nicoud, L. Benoit, C. Sensiau, and T. Poinsot. Acoustic modes in combustors with complex impedances and multidimensional active flames. *AIAA Journal*, 45:426–441, 2007.

[25] F. Nicoud and K. Wieczorek. About the zero mach number assumption in the calculation of thermoacoustic instabilities. *International Journal of Spray and Combustion Dynamics*, 1(1):67–111, 2009.

[26] M. O. Ozturkmen and Y. Ozyoruk. Investigation of a solution approach to quadratic eigenvalue problem for thermoacoustic instabilities. San Diego, CA, January 3-7 2022. AIAA SCITECH 2022 Forum.

[27] J. Pieringer, T. Sattelmayer, and F. Fassl. Simulation of combustion instabilities in liquid rocket engines with acoustic perturbation equations. *Journal of Propulsion and Power*, 25:1020–1031, 2009.

[28] T. Poinsot. Simulation methodologies and open questions for acoustic combustion instability studies. Center for Turbulence Research Annual Research Briefs, 2013.

[29] W. Schroeder, K. Martin, and B. Lorensen. *The Visualization Toolkit (4th ed.)*. Kitware, 2006.

[30] M. Schulze and T. Sattelmayer. A comparison of time and frequency domain descriptions of high frequency acoustics in rocket engines with focus on dome coupling. *Aerospace Science and Technology*, 45:165–173, 2015.

[31] G. Searby and D. Rochwerger. A parametric acoustic instability in premixed flames. *Journal of Fluid Mechanics*, 231:529–543, 1991.

DOI: 10.13009/EUCASS2023-572

[32] L. Selle, R. Blouquin, ThÃ©ron M., Luc-Henry Dorey, and W. E. Anderson. Prediction and analysis of combustion instabilities in a model rocket engine. *Journal of Propulsion and Power*, 30:978–990, 2014.

[33] C. F. Silva, I. Durán, F. Nicoud, and S. Moreau. Boundary conditions for the computation of thermoacoustic modes in combustion chambers. *AIAA Journal*, 52(6):1180–1193, 2014.

[34] C. F. Silva, F. Nicoud, T. Schuller, D. Durox, and S. Candel. Combining a helmholtz solver with the flame describing function to assess combustion instability in a premixed swirled combustor. *Combustion and Flame*, 160:1743–1754, 2013.

[35] J. C. Sisco, Y. C. Yu, V. Sankaran, and W. E. Anderson. Examination of mode shapes in an unstable model combustor. *Journal of Sound and Vibration*, 330:61–74, 2011.

[36] G. M. R. Tamanampudi, S. Sardeshmukh, W. E. Anderson, and C. Huang. Combustion instability modeling using multi-mode flame transfer functions and a nonlinear euler solver. *International Journal of Spray and Combustion Dynamics*, 12, 2020.

[37] K. Truffin and T. Poinsot. Comparison and extension of methods for acoustic identification of burners. *Combustion and Flame*, 142(4):388–400, 2005.

[38] A. Urbano, L. Selle, G. Staffelbach, B. Cuenot, T. Schmitt, S. Ducruix, and S. Candel. Exploration of combustion instability triggering using large eddy simulation of a multiple injector liquid rocket engine. *Combustion and Flame*, 169:129–140, 2016.

[39] Y. C. Yu. *Experimental and Analytical Investigations of Longitudinal Combustion Instability in a Continuously Variable Resonance Combustor (CVRC)*. PhD thesis, Purdue University, 2009.

[40] Y. C. Yu, L. A. O'Hara, J. C. Sisco, and W. E. Anderson. Experimental study of high-frequency combustion instability in a continuously variable resonance combustor. Orlando, Florida, January 5-8 2009. 47th AIAA Aerospace Sciences Meeting.

[41] Y. C. Yu, J. C. Sisco, S. Rosen, A. Madhav, and W. E. Anderson. Spontaneous longitudinal combustion instability in a continuously-variable resonance combustor. *Journal of Propulsion and Power*, 28:876–887, 09 2012.